



# Genetic algorithm optimization of defect clusters in crystalline materials



Amy Kaczmarowski<sup>a</sup>, Shujiang Yang<sup>a,1</sup>, Izabela Szlufarska<sup>a,b</sup>, Dane Morgan<sup>a,b,\*</sup>

<sup>a</sup> Materials Science Program, University of Wisconsin-Madison, Madison, WI, USA

<sup>b</sup> Department of Materials Science and Engineering, University of Wisconsin-Madison, Madison, WI, USA

## ARTICLE INFO

### Article history:

Received 14 June 2014

Received in revised form 28 October 2014

Accepted 31 October 2014

Available online 1 December 2014

### Keywords:

Genetic algorithm

Defects

Silicon carbide

Iron

Iron–chromium

Structural optimization

## ABSTRACT

A real-space genetic algorithm for the optimization of defect structures embedded in bulk crystalline materials is developed. The purpose of this method is to enable automated prediction of stable structures for a range of embedded clusters, including radiation induced defect clusters, dopant clusters, and small precipitates. The method is applied to the prediction of small interstitial clusters in cubic SiC, BCC Fe, and BCC Fe–Cr random alloys for radiation damage applications. The performance of the method is analyzed and compared to alternative techniques such as basin hopping. The technique is able to reproduce small-size defects that had been previously identified as stable or metastable structures as well as predict new mid-size defects. The structure optimization program (StructOpt) developed in this study is available under open source licensing as part of the Materials Simulation Toolkit (MAST) and can be obtained from <https://pypi.python.org/pypi/MAST>.

© 2014 Elsevier B.V. All rights reserved.

## 1. Introduction

The structure and stability of defects and defect clusters in crystalline solids control many material properties and affect performance of materials in radiation environments [1–3], electronic applications [4,5], and under deformation [6,7]. In order to understand how defects impact material performance, detailed data on both the structure and kinetics of these defects is often needed. However, determining the structure of these defects requires a systematic exploration of the potential energy surface for the system [8,9], which is a function of the number and type of atoms in the defect and their locations relative to the surrounding crystal structure.

Techniques, such as random searching [10–13], simulated annealing [14–22], minima hopping [23–26], and basin hopping [27–34] have been previously applied to the optimization of the global potential energy surface for atomic structures. However, these techniques have only rarely been applied to optimizing small defects clusters [35,36] and even then they often require many thousands of energy calculations. Furthermore, the scaling of the number of energy calculations required to find an optimal structure with the number of atoms in the defect suggests that larger

clusters may require significantly more calculations. Recent applications of genetic algorithms to similar atomic structure determination problems, namely the prediction of isolated atomic clusters [37–42], crystals [43–51], interfaces [52,53], and surfaces [54–57] have been particularly successful, and may provide some advantages in terms of speed and ability to identify promising structures as compared to other methods. Given the earlier successes, genetic algorithm approaches may provide a powerful tool for identifying defect clusters embedded in a crystalline matrix, but we are not aware of genetic algorithms having been used in this context. A genetic algorithm optimization of an embedded defect cluster faces additional challenges compared to an isolated cluster optimization due to the need to efficiently include the crystal host while focusing the optimization on the defects. Here we develop a modified genetic algorithm for the optimization of small- to mid-size interstitial and vacancy defects in bulk materials. Our approach can readily be extended to consider general precipitate structures involving arbitrary impurities and structures embedded in a host.

Due to the importance of defects in controlling effects such as swelling, hardening, and rupture in radiation environments, defect clusters in irradiated materials have been studied extensively. The availability of data on such clusters makes them ideal candidates for testing our new methodology. In particular, we will test our algorithm's ability to replicate previous results and provide new insights into defect clusters in SiC, Fe, and Fe–Cr alloys.

\* Corresponding author at: Materials Science and Engineering, University of Wisconsin-Madison, Madison, WI, USA. Tel.: +1 608 265 5879.

E-mail address: [ddmorgan@wisc.edu](mailto:ddmorgan@wisc.edu) (D. Morgan).

<sup>1</sup> Present affiliation: Deere & Company, Moline, IL, USA.

## 2. Computational methods

Genetic algorithms apply the biological notion of the evolution of a population of distinct individuals through time in order to globally optimize a given function. The application of various mating, mutation, and natural selection schemes in the genetic algorithm allows it to efficiently explore a large and complex energy landscape and arrive at a global minimum [37,44]. In this work, the individuals in the population are the different embedded defect clusters and the function being optimized is the energy. Unlike basin hopping or simulated annealing optimization approaches, genetic algorithms do not rely on the use of the stochastic Metropolis algorithm for determining the relative probability of accepting a new structure during the optimization steps. Instead, genetic algorithms optimize a population of structures, allowing them to explore multiple areas of the potential energy surface while learning from the information obtained in these many calculations to produce new structures. To date, the most effective genetic algorithms for atomic structure optimization rely on the manipulations of the real-space representation of atomic positions and compositions combined with a local relaxation of each structure in the population, as first proposed by Deaven and Ho [34].

Unlike the optimization of crystal structures or isolated atomic clusters, standard genetic algorithms optimization of the positions and types of all of the atoms in an embedded defect structure results in poor performance, slow convergence, and many unnecessary energy calculations. More fundamentally, a global minimum structure of vacancy and interstitial defects in a crystal is simply a perfect single crystal. However, such a structure is kinetically difficult to achieve in realistic materials and is therefore less interesting for the purposes of understanding the structure of defects in bulk materials. For this reason, we are interested in developing a genetic algorithm method that provides a restricted optimization, finding the stable local defect clusters, but not simply predicting a healed crystal with no defects. In order to provide bounds on the search space and to produce an efficient algorithm, the defect cluster optimization algorithm must allow for sufficient perturbations to the defect structure while preserving the majority of the surrounding material structure. There will therefore be a balance in the algorithm between how much perturbation is allowed to the bulk structure and the algorithm's efficiency and nature of the optimized structure formed. Larger perturbation will produce a more global search for stable defect clusters, but they will be slower and more likely to find an undesirable minimum that removes the defects entirely. With insufficient bounds on the search space, these low energy crystal-like structures will saturate the number of explored structures and reduce the algorithm's ability to identify the defect clusters of interest.

In order to aid in bounding the problem, the atoms in the structure are divided into three subsets as shown in Fig. 1 during the optimization. These three subsets define the defects (Set 1), a buffer region around the defects that can be altered during the evolution (Set 2), and a host crystal framework for the defect that stays approximately fixed during the optimization (Set 3). More specifically, Set 1 includes the actual defect, e.g., interstitials, dumbbells, or vacancies. These defects are identified as atoms that occupy off-lattice sites or that are missing from the crystal. For the systems analyzed in this work, the composition and number of defect atoms added as interstitials for Set 1 was explicitly specified. However, the algorithm is capable of analyzing a more open system, although this space of optimization has not yet been explored. Set two includes atoms surrounding the defect and is based either on the number of nearest neighbors or on the distance from the defect atoms in Set 1. The atoms in Set 2 are often slightly displaced from their lattice positions due to local strains from the

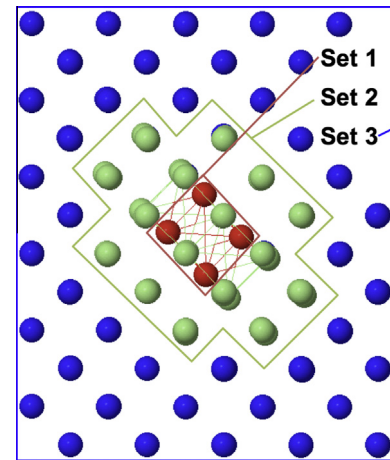


**Fig. 1.** Representation of three sets of atoms in embedded-defect optimization problem (in this case, two interstitial atoms in a bcc lattice form two dumbbells). Atoms in Set 1 are colored red, atoms in Set 2 are colored green, and atoms in Set 3 are colored blue. (For interpretation of the references to color in this figure legend, the reader is referred to the web version of this article.)

defect and the number of atoms included in this set can be very large or small depending on the system and the type of defect being analyzed. The ideal number of atoms in Set 2 depends on the anticipated perturbation to the perfect lattice structure by the presence of a particular type of defect. The definition of the size of Set 2 is key to bounding the optimization problem. Setting this size too large will result in long optimizations and the generation of a healed crystal structure with no defects, whereas setting this size too small will bias the algorithm towards searching a small solution space of the total possible configurations and possibly miss stable defect cluster structures. We will discuss below exactly how the size of Set 2 is determined. Set 3 includes those atoms that are farther away from the defect and that can be considered bulk-like atoms that should not shift significantly from their starting locations. When the actual energy calculations for each structure are performed, all three sets of atoms will interact with each other. This allows for some leniency in the definition of these sets.

These sets will change shapes and sizes as the structure adapts through the evolution of the optimization. Comparisons between each newly generated structure and the unperturbed perfect structure allow for the identification of the sets throughout the optimization. Set 1 is generally defined by identifying a defect atom by comparison to a perfect lattice using both positions and species types. In the present work we only need to identify interstitial atoms and identify an atom as an interstitial if it is greater 0.8 Å from any atom in the unperturbed perfect lattice. Set 2 is defined by all the atoms that are within some cutoff, denoted  $r_{2c}$ , of Set 1 in the structure being optimized. This cutoff is specified by a simple formula that depends on the number of atoms in Set 1 and lattice parameter. It is set in the initial first step of the genetic algorithm and held constant throughout the simulation. The formula for  $r_{2c}$  is given for each case in line 4 of Table 1. The formulas are based on the following logic. First,  $r_{2c}$  is assumed to scale with the lattice parameter  $a$  so that a simple scaling of the lattice does not alter the size of Set 2. Second  $r_{2c}$  is assumed to scale as  $n^{1/3}$  (where  $n$  is the size of Set 1) as this will approximately scale the cutoff in proportion to the linear dimensions of Set 1. We found that simple setting  $r_{2c} = n^{1/3} \cdot a$  worked quite well for about half our cases. For the difficult to converge cases of the Laves phases discussed later, we found that a larger  $r_{2c}$  value was needed. While there are many possible ways to increase the cutoff we arbitrarily chose to increase the scaling with  $n$  to be  $n^{2/3}$ . We note that many

**Table 1**  
Parameters for genetic algorithm optimizations. Descriptions for these parameters as well as the values and descriptions for the default parameters not listed here can be found in Section 2 of this document as well as the StructOpt documentation available at <https://pypi.python.org/pypi/MAST>.

Genetic algorithm parameters	SiC	Fe (BCC-like clusters)	Fe (Laves clusters)	Fe–Cr (Laves clusters)
Number of individuals in population	50	50	50	50
Number of atoms in bulk system	216	1024	686	686
Initiation structure of Sets 1 + 2	Random dumbbells	Random positions for Set 1	Random positions for Sets 1 and 2	Random positions for Sets 1 and 2
Formula for size of Set 2 cutoff ( $r_{2c}$ )	$n^{1/3} \cdot a$	$n^{1/3} \cdot a$	$n^{2/3} \cdot a$	$n^{2/3} \cdot a$
$n$ = # of atoms in Set 1				
$a$ = lattice parameter				
Crossover fraction	0.8	0.8	0.8	0.8
Crossover method	Random rotate–cut	Random rotate–cut	Random rotate–cut	Random rotate–cut
Crossover selection scheme	Tournament	Tournament	Tournament	Tournament
Mutation fraction	0.2	0.2	0.2	0.3
Mutation options (all equal probability)	Move, rotate, quench (probability of quench increased to 66% of all mutations)	Move, rotate, quench	Move, rotate, quench	Move, rotate, permute, quench, basin hop permute
Natural selection scheme	FUSS	FUSS	FUSS	FUSS
Additional bias	Si atom lattice site fitness bias	None	None	Constrain relative position of Cr atoms

other choices for these larger  $r_{2c}$  values might work equally well or even better. Once these sets have been defined for each individual (structure) in the population, the mating and mutations of the structure can be applied specifically to Sets 1 and 2. This procedure allows for a targeted evolution of the defect structure while minimizing the impact of the evolution on the surrounding lattice.

There are a few methods for generating the initial defect structures depending on how much one wants to bias the algorithm to search particular configurations. The basic method involves the random generation of only the atoms in Set 1. For instance, if the optimization case was targeting a five-interstitial structure, then five interstitial atoms of the desired composition would be generated at random positions within a user-defined region. Alternatively, one could also generate various arrangements such as five randomly oriented dumbbells in order to reduce the number of calculations if the defect structures are known to prefer dumbbell arrangements. While the specific defects examined in this work were constrained to have a fixed number of interstitials (and in some cases a fixed composition of interstitials), the algorithm does have the potential to search configurations with variable number and composition of the atoms in the defect. The most robust method for generating individual defect structures to search the widest number of configurations is to randomly generate the atoms in Sets 1 and 2. This generation method is particularly suited for optimizing structures that may result in large deformations to the local lattice structure as it increases the likelihood that such highly deformed structures will be found and survive given a limited population size.

The defect optimization algorithm utilizes a variation on the cut and splice mating crossover procedure proposed by Deaven and Ho [34] for the optimization of clusters. In this operation, the atoms in Set 1 are treated as a cluster and the maximum and minimum  $x$ ,  $y$ , and  $z$  coordinates of all the atoms in the set define a spatial region bounding the Set 1. Then a random point and a randomly oriented plane passing through this point are chosen within the bounding region. If this plane divides the cluster into two sets of atoms it is used for the next step, and if not another plane is selected. The final selected plane is then used to perform the cut and splice mating crossover procedure. Through these crossovers, the number of defected atoms and typically the overall composition of the system are maintained. Cut and splice operations that do not maintain these conditions are simply not executed and another cut and splice attempt is made until one that does maintain the desired properties is obtained. For each generation, only a fraction of the

population will undergo these mating procedures with the pairs of structures selected using a tournament selection scheme as described in [37].

After the crossovers, a small fraction of the population undergoes mutations. Several different types of mutations (with varying complexity) can be applied to the structure. The simplest mutations consist of random movements of atoms, random rotations of a subset of atoms, and random permutations of atom types within a structure. Additionally, the algorithm allows for the use of more complicated mutations that borrow from other optimization techniques in order to make it more effective. Possible mutations include rapid molecular dynamics quenches of the defected structure and short basin hopping minimizations. Examples of the use of these mutation methods will be discussed for some of the systems analyzed in this work.

After the crossovers and mutations, the new defect structure is re-embedded in the perfect bulk structure (atoms from Set 3) and all of the atoms are locally relaxed at fixed volume using a conjugate gradient relaxation or a molecular dynamics quench. Quenching can be used either as a mutation and applied only to randomly selected structures throughout the optimization, or as a local optimizer and applied to all of the structures in the optimization. The effectiveness of the quench in either context depends on the system being optimized. The number of calculations required by the algorithm is significantly reduced by the use of a local optimizer as it reduces the reliance on the genetic algorithm to identify local minima, which is rather inefficient. The reader is referred to [34] for a full description of the importance of this local optimizer. These atomistic simulations are carried out by interfacing our algorithm with the Large-scale Atomic/Molecular Massively Parallel Simulator (LAMMPS) [58] molecular dynamics code.

Once all the individuals in a population have been locally minimized and their energies have been evaluated, a selection scheme is used to determine which individuals will survive to the next generation. As with crystal optimization problems, the embedded defect algorithm will suffer from a reduction in the diversity of the population as structures locally relax into equivalent or similar structures. In order to overcome this problem and maintain the diversity of the population, we use a combination of the energy predator and the fixed uniform selection scheme (FUSS) as described in Ref. [59]. The energy predator assumes that configurations with energies that are within a certain tolerance of each other are structurally similar and can therefore be removed from the population. Iteration of the mating and mutation schemes acting

on the population through several generations lead to identification of the best guess of the global minimum defect structure, as well as other closely competitive defect structures.

The genetic algorithm optimization is viewed as converged and terminated after no new lower energy structures have been identified for some number of generations,  $n_{\text{conv}}$ . For this work we chose  $n_{\text{conv}} = 50$  generations, however, the user can set the exact number of generations and there is no set standard for all types systems for the optimal value of  $n_{\text{conv}}$ . As  $n_{\text{conv}}$  can be set to various values the total number of steps required to reach convergence is not an intrinsic value of the algorithm and therefore we do not use it in our assessment of the algorithms calculation requirements. Instead we focus on the number of calculations required to first identify what we believe to be the ground state, which is determined to be the ground state by running to full convergence including the final  $n_{\text{conv}}$  steps. In other words, only the number of calculations required to first identify the minimum energy structure is presented, not any additional steps taken to assure that the structure is in fact the minimum energy structure. We further note that despite our best efforts, we cannot be sure that the lowest energy structures found here are in fact the true ground state structures for our given potentials and optimization constraints. However, to avoid constantly qualifying our reference to these states, we will refer to what we have predicted with our fully converged algorithm as the lowest energy structures as simply the “ground state structures”, and the reader should keep in mind that further research could at some point yield more stable structures.

There are some additional important limitations to the genetic algorithm optimization technique presented here. First, the genetic algorithm does not account for any possible kinetic barriers to forming a specific defect. While a structure may have a low energy, diffusion processes and energies of intermediate steps may prevent the structure from occurring experimentally. Additionally, the present genetic algorithm optimizes only the potential energy of a structure and all of the calculations are performed at zero Kelvin (0 K). Nature, of course, will optimize to form defects with the lowest free energy. If thermal excitations significantly alter which defects are stable, then these finite temperature effects will not be represented. While the genetic algorithm could in theory be expanded to optimize free energies if they can be practically calculated (e.g., by including vibrational free energy contributions), no efforts in this direction have been pursued here. We also note that our predictions are subject to any inaccuracies in the Hamiltonian (e.g., due to the use of interatomic potentials rather than more accurate *ab initio* methods). Finally, we reiterate that in general, a genetic algorithm cannot guarantee that a structure is a global minimum, especially in our case as the results can depend on the constraints applied to the search space by limiting the size of the atoms in Sets 1 and 2. However, a genetic algorithm can provide new insights into low energy structures and in practice finds the desired minima for the cases considered here.

The genetic algorithm for defect structure optimization described here is implemented in the general atomic Structural Optimization (StructOpt) program. StructOpt is available under open source licensing as part of the Materials Simulation Toolkit [60] and can be obtained from <https://pypi.python.org/pypi/MAST>. StructOpt is built using the Atomic Simulation Environment [61] in python. When using the StructOpt code, please cite the references given in the MAST citation file, which is generated automatically when MAST is run. The optimizations presented in the following sections were conducted mostly using the default parameters in StructOpt. The important parameters or those that differed from the default values given in Table 1 are described in detail when the related optimization is discussed below. It should be noted that these parameters were not formally optimized for best performance but rather are the result of trial and error. Full example

input files for the optimizations described here can be found in the [Supplemental Material](#) of this publication. Please refer to the StructOpt documentation (also available at <https://pypi.python.org/pypi/MAST>) for more detailed explanations of the code features and default parameters.

### 3. Results

#### 3.1. SiC interstitial clusters

Understanding defects in SiC is important because of the use of this material in semiconductor electronics, where defects can degrade device performance, as well as its potential use in radiation environments (e.g., in TRISO nuclear fuels [62]) where irradiation creates defects that can alter mechanical and structural properties. In order to test the performance of the algorithm in a periodic ceramic structure, the genetic algorithm was used to analyze carbon interstitials in  $\beta$ -SiC. An exhaustive analysis of stable defect cluster configurations consisting of 1–6 interstitials have been previously reported by [35,36], who used the basin hopping and simulated annealing optimization techniques. These published structures can be used for comparison to the genetic algorithm predicted structures in order to assess the performance of the algorithm. The studies by Jiang et al. utilized the Environment-Dependent Interatomic Potential (EDIP) for SiC developed by Lucas et al, which potentially shows a good qualitative agreement with DFT calculations of carbon defects up to about four interstitials [63]. Additional investigations of SiC defects can be found in Refs. [64–71]. We note that Jiang et al. intentionally constrained their search to yield structures with only C interstitials. Therefore, in order to match the results from Jiang et al. [35,36] and to test the performance of our algorithm, we, too, constrain our to structures with C interstitials. To impose such constraints, we bias the algorithm towards searching a solution space where Si atoms were constrained to remain on lattice sites. This constraint was necessary to avoid finding structures with significant Si interstitial content, as these occurred in unconstrained optimizations even when starting from only excess C interstitials. The on-lattice constraint for Si was forced by introducing a fitness penalty of 50 eV/Si for individuals with interstitial Si atoms. The Si atom is considered an interstitial if it is displaced from a lattice site by more than 0.5 Å. Additionally, it was found that because of the existence of many local minima in the EDIP potential, the use of quench mutations in identifying the stable configurations in SiC was essential. The parameters used for the SiC optimizations are given in Table 1.

##### 3.1.1. SiC results

The low energy configurations and formation energies for up to 6 carbon interstitials in SiC identified by the genetic algorithm are shown in Fig. 2 and their energies summarized in Fig. 3. The energies are given per an interstitial and are relative to the energy of the perfect cubic SiC structure (lattice parameter = 4.364 Å). The small-scale structures show good agreement with the structures identified in previous work [35,36] using the EDIP potential. For instance, the algorithm correctly identifies the low energy bond-center positions between Si and C atoms of the di-interstitial, the tri-interstitial triangular ring, as well as the split-interstitial tetra-interstitial structure and hexa-interstitial structure identified in previous studies [35,36,63,65,69]. However, for the penta-interstitial case, the carbon atoms begin to form a small three-dimensional pentagonal ring. This structure has not been shown in previous studies and has a slightly lower energy than the most stable structure previously identified with the EDIP potential in [36]. Specifically, the 5 carbon interstitial cluster identified by the genetic algorithm has a formation energy of 2.74 eV/int



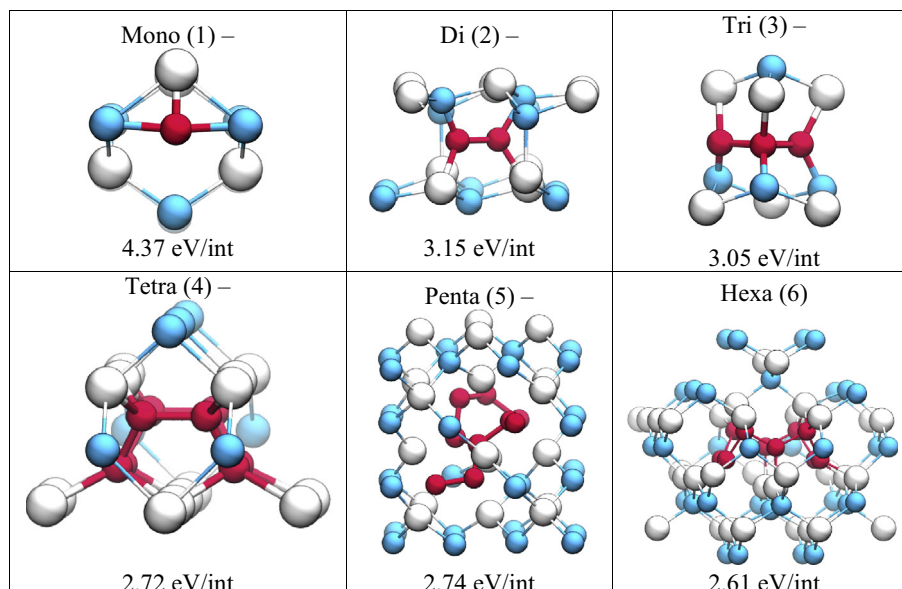


**Fig. 2.** Low energy configurations of SiC. White atoms are Si, blue atoms are C atoms on lattice sites, red atoms are C atoms off lattice. (For interpretation of the references to color in this figure legend, the reader is referred to the web version of this article.)

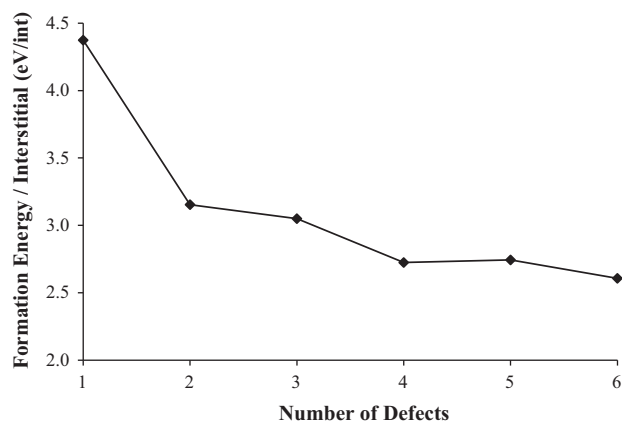


**Fig. 3.** Formation energy for carbon interstitials in SiC as predicted by genetic algorithm with EDIP potential.

whereas the defect identified in [36] is a chain-like arrangement of carbon dumbbells and has a formation energy of 2.75 eV/int. The successful identification of C interstitial cluster structures equivalent to, or even slightly more stable than, those found for the same EDIP potential in previous work [35,36] demonstrates the ability of the genetic algorithm to thoroughly explore the potential energy landscape. The structures and their formation energies are shown in Fig. 3. We note that the stability of these defect structures using more accurate Density Functional Theory (DFT) calculations is unconfirmed, and specifically the 5 interstitial case may not be more stable than that identified by Jiang et al. [35,36] for a full DFT Hamiltonian.

The performance of the algorithm in the prediction of the carbon clusters in SiC can be seen in Fig. 4. Plotted in Fig. 4 is the average number of calculations required to first identify the stable structure as well as the standard deviation in the number of calculations for optimizations conducted with differing random number seeds. In general, the results for the different optimizations are typically within 5–10 generations of one another for the approximately 5 different optimizations performed for each defect. The algorithm required 50–100 generations for convergence and

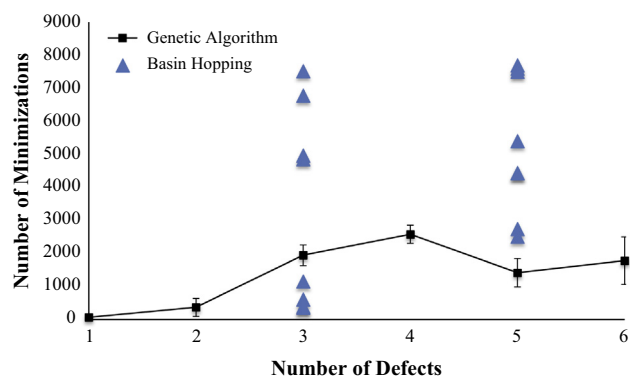


**Fig. 4.** Genetic algorithm performance for SiC interstitials in comparison with basin hopping performance – average number of energy minimizations required to identify the minimum energy structure. There error bars on the genetic algorithm data represent one standard deviation in the number of calculations for optimizations found by approximately five optimizations with differing random number seeds and in some cases the error bars cannot be seen as they are smaller than the symbol. The number of calculations can be divided by the population size of 50 to calculate the number of generations required for the genetic algorithm.

1000–2000 total calculations, where one calculation can consist of either a conjugate gradient or quench local relaxation. The relatively similar total number of calculations required for different numbers of atoms in the cluster is very encouraging and suggests that genetic algorithms may be practical for much larger clusters as well. Also shown in Fig. 4 is the performance of a simple basin hopping optimization similar to that used in [36] for the 3 and 5 interstitial cases. The data shows the number of calculations required to identify the structures shown in Fig. 2 for different starting configurations of carbon dumbbells and random number seeds. It can be seen that some of the basin hopping algorithm runs were able to outperform the genetic algorithm for defect structures while others were significantly worse. A more tuned basin hopping algorithm may be able to more consistently outperform the genetic algorithm, so this cannot be taken as proof that the genetic algorithm is clearly better or worse than the basin hopping approach. However, the genetic algorithm did yield somewhat more stable clusters not found in basin hopping searches and did so with a

relatively minor amount of computation (the total time for 2000 steps is approximately 35 h on one state of the art compute core). It should be noted that, similar to the basin hopping method, the number of generations required to identify the minimum energy structure fluctuates between different optimizations, especially if the optimization relies more heavily on the use of mutations to identify the ground state structure. The data shown in Fig. 4 represents the number of generations to first find the stable carbon cluster ground states we have identified. However, in the usual case where the ground state is not known, more calculations are required to ensure that the algorithm has fully searched the potential energy space and that the identified structure is truly the ground state structure. As described above in the methods section, we typically require a structure remain as the ground state for 50 generations before terminating the optimization.

### 3.2. Fe interstitial clusters

Small and mid-scale defect clusters in BCC-Fe have been thoroughly studied using a variety of techniques due to the widespread use of Fe and Fe-based alloys in radiation environments for nuclear reactors [72–83]. From these studies, two general types of stable structures for Fe self-interstitial atoms have been identified. The two structures correspond to what are essentially configurations of mostly parallel interstitial dumbbells embedded in the BCC lattice (which we will refer to as “BCC-like” structures as they are primarily defects within a BCC host) and C15 Laves phase structures [76]. Therefore, these clusters provide an interesting test case for evaluating the performance and flexibility of the genetic algorithm for defects. The Fe defect clusters in this analysis were evaluated using the Ackland–Mendelev embedded atom potential [84] that has been shown to provide good agreement to DFT results for small-scale self-interstitial atom defect clusters in Fe [75]. However, as with the other studies in this work, no validation or comparison to DFT results has been done here.

The parameters shown in Table 1 under the Fe column were used to optimize within the search space of the BCC-like structures, which largely maintain the structure of the BCC host even within the defect cluster. However, in order to explore the Laves phase structure for Fe self-interstitials three types of adjustments were needed to the parameters used in the BCC-like structure search. These altered parameters are given in Table 1 under the Fe Laves column. First, the choice for the sizes of each of the three atom sets must be carefully considered. For the previous example of carbon interstitials in SiC, it was unlikely that many of the lattice atoms would be disturbed by the small size of interstitials considered. However, for the problem of self-interstitial Laves phases in Fe, many lattice site atoms can potentially be displaced, as even two interstitials in the Laves phase structure would result in an additional 12 displaced lattice atoms. In addition to the atom set size parameters, the method of defect structure generation also needed to be changed. For structures that may result in large perturbations to the host lattice, such as the Laves phase structures, initializing the population with atoms in Sets 1 and 2 randomized can result in an increased likelihood of identifying low energy structures. Initializing the population with these randomized structures is more effective than relying on random mutations and crossovers to produce more lattice displaced structures because of the difficulty in maintaining the diversity of the population in a genetic algorithm and the potentially high energy nature of the transition structures between the dominantly BCC structure and the optimal Laves structure. A third alteration to the parameters to assist in the identification of defects with increased amounts of off lattice site atoms is to increase the concentration of defects in the simulated periodic cell by decreasing the supercell size or number of atoms in Set 3 (the bulk region). While the detailed mechanism of why decreasing

the number of BCC structure atoms in Set 3 improves the algorithms performance is not clear, it is likely that this improvement is due to the ability for the defect to interact with its mirror images through strain.

#### 3.2.1. Fe results

The genetic algorithm predictions for the low energy structures for 1–10 self-interstitial atoms in Fe and their corresponding formation energies are shown in Fig. 5 for the parallel arrangements and Fig. 6 for the Laves phase structures, and the formation energy data is summarized in Fig. 7. The energies are given per an interstitial and are relative to the perfect BCC Fe structure (lattice parameter = 2.855 Å, as given by volume optimization with the Ackland–Mendelev potential). The algorithm was able to identify the same ground state defect structures in Fe that had been reported in previous studies on self-interstitial clusters [76,77] carried out using the same potential. It should be noted that other potentials and DFT methods show that the ground state for the three-interstitial case is also a Laves structure. However, the inability for the genetic algorithm to predict this structure is a limitation in the potential not an issue with the genetic algorithm. Additionally, the Ackland–Mendelev potential used in this study only weakly stabilizes the Laves phase structures over competing BCC-like structures compared to other potentials and DFT. With the potential used in [76] and DFT methods, the C15 structures are far more stable than shown here in Fig. 7. The identified configurations from the genetic algorithm for cluster sizes 1–3 are coupled arrangements of dumbbells aligned in the [1 1 0] direction. For clusters of four interstitials or more, the genetic algorithm captured the highly stable ground state C15 Laves phase structures. Additionally, by controlling the parameters of the genetic algorithm, the experimentally more common parallel configurations for larger cluster sizes were also identified.

The performance of the algorithm is summarized in Fig. 8. Plotted here is the average number of calculations required to identify the minimum energy structure from five independent optimizations for the BCC-like structures and three optimizations for the Laves structures as well as the standard deviation of the results. From the figure, it can be seen that the algorithm identifies the stable configuration for small clusters of sizes 1–3 within 1–2 generations while larger clusters require between 10 and 20 generations to identify the proposed global minimum for BCC-like structures. Fig. 8 also demonstrates the added computational cost for identifying the Laves structures. This result is consistent with the larger solution space the genetic algorithm must search in order to identify structures with more highly disturbed lattice atoms. The algorithm is able to identify the proposed minimum energy structure for up to 10 self-interstitial atom configurations within roughly 6500 local energy minimization calculations, which is approximately 130 generations each with populations of 50 individual defect clusters. As noted for the SiC performance in Section 3.1.1, after an initial increase we see an encouraging stabilization of the number of steps required to find the minimum energy structure vs. number of interstitials.

#### 3.3. Fe–Cr interstitial clusters

As Fe–Cr alloys form the basis for many steels used or being considered for nuclear reactors, the understanding of defect motion and structure in these metals has been a focus of many studies. Fe–Cr alloy interstitials with varying Cr concentrations have been analyzed previously for mono-interstitials using set of predetermined configurations [85]. For consistency with these analyses, we use the modified concentration-dependent embedded atom method (CDEAM) potential version 2 developed by Stukowski et al. [86] to evaluate the energies of the defects. While this

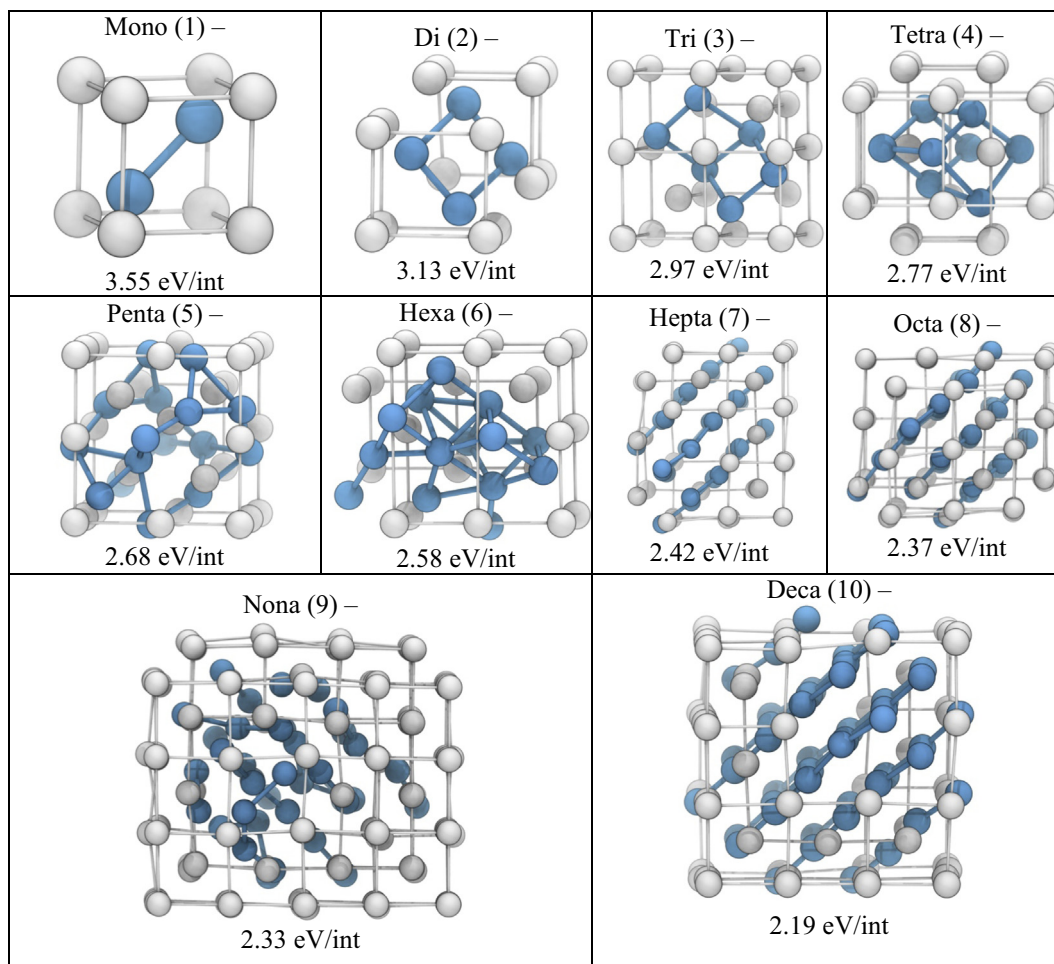


**Fig. 5.** Fe self-interstitial atom configurations (1–10) and corresponding formation energies for BCC-like structures as identified by the genetic algorithm. White atoms represent Fe atoms on lattice sites and blue atoms represent Fe atoms off lattice. (For interpretation of the references to color in this figure legend, the reader is referred to the web version of this article.)

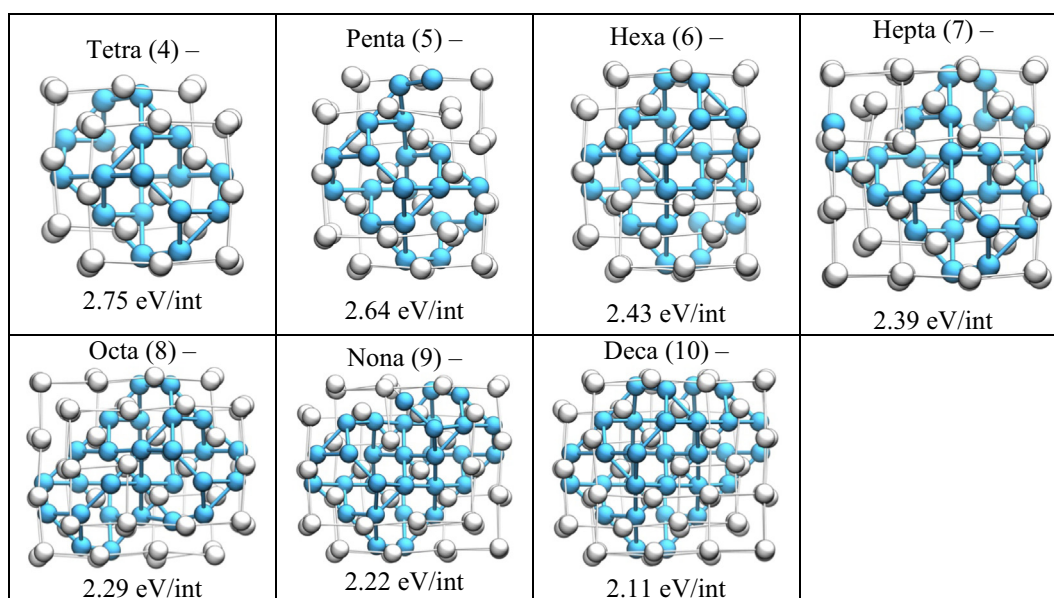


**Fig. 6.** Fe self-interstitial atom configurations (for 4–10 interstitials) for the stable Laves structures as identified by the genetic algorithm. White atoms represent Fe atoms on lattice sites and blue atoms represent Fe atoms off lattice. No Laves phase structures are found for three or fewer interstitials. (For interpretation of the references to color in this figure legend, the reader is referred to the web version of this article.)

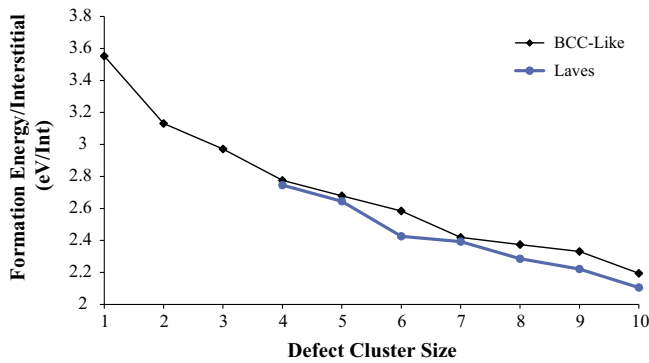


Fig. 7. Defect formation energy for Fe interstitials for both the BCC-like and C15 Laves structure configurations, taking the lowest energy structure of each type predicted by all the optimizations.

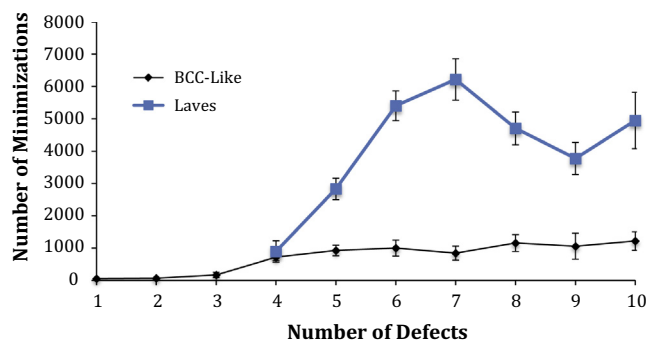


Fig. 8. Algorithm performance for Fe interstitials – average number of energy minimizations required to identify minimum energy structure. The error bars represent one standard deviation in the number of calculations for optimizations found by 3–5 optimizations with differing random number seeds and in some cases the error bars cannot be seen as they are smaller than the symbol. The number of calculations can be divided by the population size of 50 to calculate the number of generations required.

potential shows a better qualitative agreement with density functional theory predictions of stable defects than the original concentration dependent embedded-atom model, the modified potential occasionally predicts overly strong local Cr–Cr repulsion and weak long-range Cr–Cr interactions. Additional analysis of defects in the Fe–Cr system can be found in the following Refs. [87–92].

Similar to the Fe system, Fe or Cr interstitials in Fe–Cr alloys cause large lattice distortions. Therefore, we include the alterations to the genetic algorithm parameters needed to obtain the C15 Laves phase for Fe as discussed in Section 3.2 in the analysis of the Fe–Cr system. The Fe–Cr system provides an opportunity to analyze the performance of the algorithm for embedded clusters for a multi-component system. However, because Fe–Cr forms a random alloy, optimization of defect structure needs to be constrained. Otherwise, the algorithm will attempt to organize the positions of all of Cr atoms in the simulation cell rather than focusing on the configuration of the embedded defect. While such an optimization over all possible Cr positions is achievable in theory, we found that the algorithm was very slow to converge and the majority of the calculations were spent on rearranging Cr positions on the lattice rather than identifying the defect structure of interest. In order to direct the algorithm towards the atoms and composition of the defect structure, the interstitial atoms were introduced in a pure BCC Fe crystal and between 1 and 5 Cr atoms were randomly placed within Sets 1 and 2, which are described in Section 2. As the population evolved, we constrained the Cr atoms to remain within Sets 1 or 2 with no compositional swapping with

Set 3. If a Cr atom was found outside of Sets 1 or 2 due to the evolution of the structure, the Fe atom in Sets 1 or 2 that was nearest to the Cr atom was swapped with the Cr. Sets 1 and 2 combined contain roughly 100 atoms as opposed to the 1000 atoms or more available in Set 3, thus greatly reducing the search space for the algorithm. In order to further improve the performance of the algorithm in identifying Cr location, a basin hopping permutation mutation was also used. This mutation employs a short 20-step basin hopping algorithm to alter the Cr positions in Sets 1 and 2.

### 3.3.1. Fe–Cr results

The lowest energy structures produced by the genetic algorithm for 1–5 interstitial atoms with 1–5 local Cr atoms are shown in Fig. 9 and are summarized in Fig. 10. The energies are given per interstitial and are calculated from the following equation:

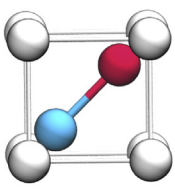
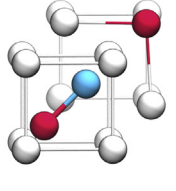
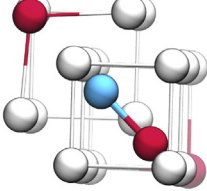
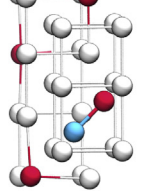
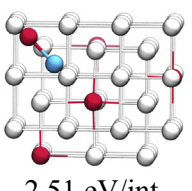
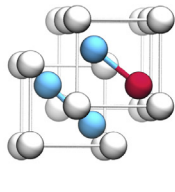
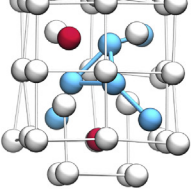
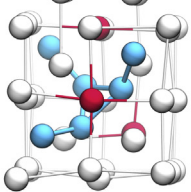
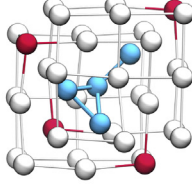
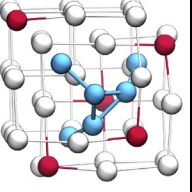
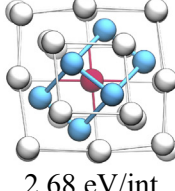
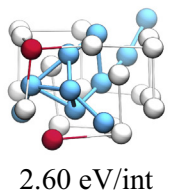
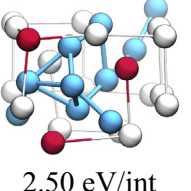
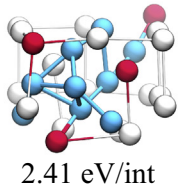
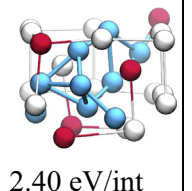
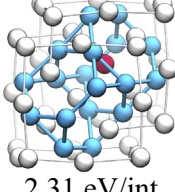
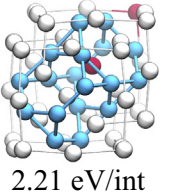
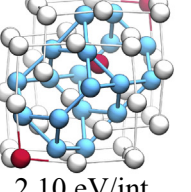
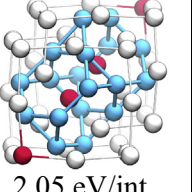
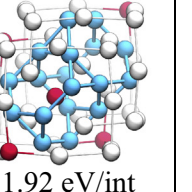
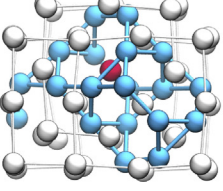
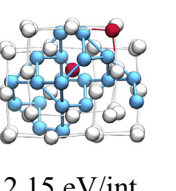
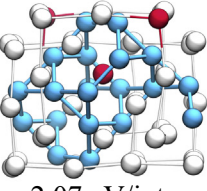
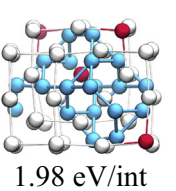
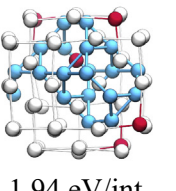
$$E_f = E_d - \sum n_i \mu_i \quad (1)$$

where  $E_d$  is the energy of the defected structure,  $n$  is the number of atoms of a given type, and  $\mu$  is the cohesive energy per atom of BCC Fe and BCC Cr.

In general we find that Cr rarely enters the defects to form mixed dumbbells, and then only up to one Cr. For the mono-interstitial case, the low energy state consists of a mixed Fe–Cr  $\langle 110 \rangle$  dumbbell with additional Cr atoms arranged in the vicinity of the dumbbell. It is somewhat unsatisfying that the Cr arrangement we obtain does not have an obvious intuitive rationalization. However, further exploration of different Cr arrangements of the Cr on the lattice did not yield any lower energy structures. For the di-interstitial case, the mixed dumbbell persists only for the single Cr atom structure. Two Cr atoms nearby the defect allow for the stability of a non-parallel arrangement of  $\langle 110 \rangle$  Fe dumbbells, with no Cr as an interstitial. For reference, the lowest formation energy identified for a mixed parallel dumbbell is about 10 meV/int higher than the non-parallel pure Fe dumbbell configuration. To stabilize the di-interstitial defect cluster, the Cr atoms arrange themselves in first and second nearest neighbors, often along the diagonals of the dumbbells, as shown in Fig. 9. For the tri-interstitial case, the single Cr atom exists along with parallel pure Fe  $\langle 110 \rangle$  dumbbells. Increasing the number of local Cr atoms allows for the stability of non-parallel  $\langle 110 \rangle$  and  $\langle 111 \rangle$  dumbbells with Cr atoms in first and second nearest neighbors, but still does not lead to formation of mixed dumbbells. Similarly to the Fe clusters, the C15 Laves phase structures become stable after approximately four interstitial atoms for the CDEAM potential, and therefore we show the Laves structures for four or more interstitials. In general, the Cr atoms tend to align along the central diagonal ( $\langle 111 \rangle$ ) direction through the Laves structure. From Fig. 10, it can be seen that the presence of Cr atoms tends to stabilize the defect clusters and reduce the formation energy of the defect. While the structures shown in Fig. 9 are the lowest energy embedded defects identified with the genetic algorithm for the CDEAM potential, limitations of the potential mean that these interstitial structures may not be the most stable structures predicted with more accurate Hamiltonians (e.g., ab initio methods) or be the most stable structures for real Fe–Cr alloys. Furthermore, the ability of these embedded clusters to form in nature will depend on kinetic factors and the availability of Cr atoms. However, the range of structures identified by the algorithm and the discovery of highly stable complex non-parallel clusters for even small numbers of defects demonstrates the algorithm's ability to search a wide range of configurations.

The performance of the algorithm in the optimization of the Fe–Cr embedded defects is shown in Fig. 11. It can be seen that there is an increase in the number of required calculations as the number of Cr atoms in the defect increases. The cause of this increase can be linked to the fact that the movement of Cr atoms between



# of Cr Atoms \ # of Defects	1	2	3	4	5
1	 3.15 eV/int	 2.94 eV/int	 2.77 eV/int	 2.63 eV/int	 2.51 eV/int
2	 2.86 eV/int	 2.73 eV/int	 2.60 eV/int	 2.53 eV/int	 2.46 eV/int
3	 2.68 eV/int	 2.60 eV/int	 2.50 eV/int	 2.41 eV/int	 2.40 eV/int
4	 2.31 eV/int	 2.21 eV/int	 2.10 eV/int	 2.05 eV/int	 1.92 eV/int
5	 2.22 eV/int	 2.15 eV/int	 2.07 eV/int	 1.98 eV/int	 1.94 eV/int

**Fig. 9.** Low energy Fe–Cr interstitial clusters with varying Cr concentrations. White atoms are Fe atoms on lattice sites, blue atoms are interstitial Fe atoms, and red atoms are Cr atoms. (For interpretation of the references to color in this figure legend, the reader is referred to the web version of this article.)

lattice sites is best controlled through permutation mutations. Therefore, the Fe–Cr simulations are more heavily reliant on mutations than the Fe or SiC simulations. It is possible that the performance of the algorithm can be improved by either increasing the probability of a permutation mutation to occur or by further reducing the number of atoms in Set 2 and the number of sites accessible to the Cr atoms.

#### 4. Discussion

The modified genetic algorithm proposed in this work for the optimization of defects in crystalline materials is shown to be

effective in identifying low energy stable interstitial configurations by comparison to results of previous searches with different methods. The algorithm can be applied to a variety of systems and defects of various sizes. The number of calculations required to find the stable ground states does not appear to increase significantly as the number of defects increases, at least within the range of defect cluster sizes studied here (up to 5–10 interstitials). The search space of the algorithm is tunable and capable of identifying both compositionally and structurally variant defects through the control of fitness-based biases as well as the atoms used in the mutations and crossovers. Reducing the search space in this way allowed the algorithm to identify the stable arrangements of small

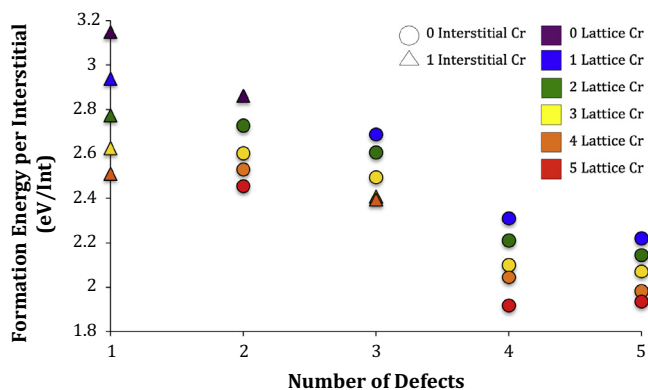


**Fig. 10.** Defect formation energies and Cr content for Fe–Cr interstitials. The symbol type gives the number of interstitial Cr and the color gives the number of Cr atoms on lattice sites. For example, the filled blue circle for four defects represents the energy of a four interstitial cluster with one lattice Cr and zero interstitial Cr. (For interpretation of the references to color in this figure legend, the reader is referred to the web version of this article.)

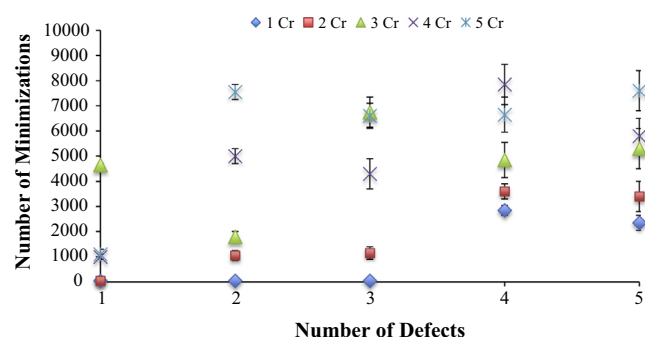


**Fig. 11.** Algorithm performance for Fe–Cr interstitials is shown by the average number of energy minimizations required to identify the minimum energy structure. The error bars represent one standard deviation in the number of calculations for optimizations found by 3–5 optimizations with differing random number seeds and in some cases the error bars cannot be seen as they are smaller than the symbol. The number of calculations can be divided by the population size of 50 to calculate the number of generations required.

numbers of carbon interstitials in SiC, either as effectively or better than previous optimizations. The algorithm also found very stable clusters for Fe and Fe–Cr exploring both BCC-like and Laves phase structures in different areas of the search space. We therefore find that with some modifications to the algorithm, such as seeding the population and tuning parameters to be more system specific, the approach can be applied to systems with large lattice atom distortions, small lattice atom distortions, and varying composition.

While the structures shown in this current study are limited by the reliability of the potentials used for each system, the performance of the algorithm demonstrates that the minimum energy structures can typically be identified within approximately 10,000 local energy relaxation calculations (either conjugate gradient or quenched molecular dynamics) for structures with relatively larger lattice atom distortions among the sets considered here. This performance improves for structures with relatively smaller lattice atom distortions among the sets considered here, which require approximately 5000 calculations. This scale of calculations is quite trivial for interatomic potentials and, while very large, is presently (or will soon be) achievable for more accurate Hamiltonians such as Density Functional Theory (DFT), provided the unit cell sizes can be kept tractable. DFT-based genetic algorithms have already been used in the optimization of other types of atomic structures [93]. Furthermore, a reduction in the number of required

calculations may be achieved by seeding the population with previously identified minima defect structures (e.g., the starting structures for a  $(n)$ -interstitial calculation could be initiated from optimized  $(n - 1)$ -interstitial structures with one extra interstitial added), as opposed to the random initial population presented in this study. Additional improvements in the efficiency of the genetic algorithm may be possible by replacing the simple energy-based predator used in this implementation with predators based on structural features, such as crystal fingerprints similar to those used in crystal structure genetic algorithm optimizations [45,46], in order to prevent the re-evaluation of structurally similar defects. Overall, the genetic algorithm optimization technique presented in this study appears to be a powerful method for identifying defect clusters using a range of Hamiltonians.

## Acknowledgments

A. Kaczmarowski would like to acknowledge the Sandia National Laboratories Critical Skills Masters Program for their support of her research. A. Kaczmarowski was responsible for aspects of the idea generation, the code development, and led the manuscript writing. D. Morgan would like to acknowledge support provided by NSF Software Infrastructure for Sustained Innovation (SI<sup>2</sup>), award no. 1148011. D. Morgan was responsible for initiating and leading the project, reviewing code development, and reviewing the manuscript. MAST was developed at the University of Wisconsin-Madison under NSF award no. 1148011. I. Szlufarska would like to acknowledge support by the U.S. Department of Energy, Office of Basic Energy Sciences Grant No. DE-FG02-08ER46493. I. Szlufarska was responsible for discussing aspects of clusters in SiC and reviewing the manuscript. S. Yang would like to acknowledge support by University of Wisconsin Materials Research Science and Engineering Center (DMR-1121288). S. Yang aided the early development of the genetic algorithm approach through discussions and assistance identifying relevant literature. The authors gratefully acknowledge use of facilities and instrumentation supported by the University of Wisconsin Materials Research Science and Engineering Center (DMR-1121288). We thank Tam Mayeshiba, Dr. Chao Jiang and Dr. Mihai-Cosmin Marinica for helpful conversations and sharing their data files.

## Appendix A. Supplementary material

Supplementary data associated with this article can be found, in the online version, at <http://dx.doi.org/10.1016/j.commatsci.2014.10.062>.

## References

- [1] R. Averback, T.D. de La Rubia, *Solid State Phys.* 5 (1997) 281–402.
- [2] T. Muroga, M. Gasparotto, S. Zinkle, *Fusion Eng. Des.* 62 (2002) 13–25.
- [3] G. Odette, G. Lucas, *JOM* (July 2001) 18–22.
- [4] A. Bongiorno, L. Colombo, *EPL (Europhys. Lett.)* 50 (5) (2000) 608–614.
- [5] S. Dutta, S. Chattopadhyay, A. Sarkar, M. Chakrabarti, D. Sanyal, D. Jana, *Prog. Mater. Sci.* 54 (1) (2009) 89–136.
- [6] P. Gumbsch, R. Schroll, *Intermetallics* 7 (1999) 447–454 (July 1998).
- [7] J. Li, A.H.W. Ngan, P. Gumbsch, *Acta Mater.* 51 (19) (2003) 5711–5742.
- [8] D.J. Wales, *Energy Landscapes: Applications to Clusters, Biomolecules and Glasses*, Cambridge University Press, New York, 2003, pp. 192–352.
- [9] D.J. Wales, T. V. Bogdan, *J. Phys. Chem. B* 110 (42) (2006) 20765–20776.
- [10] C.J. Pickard, R.J. Needs, *J. Phys.: Condens. Matter* 23 (5) (2011) 053201.
- [11] C.J. Pickard, R.J. Needs, *Phys. Status Solidi* 246 (3) (2009) 536–540.
- [12] H.A. Scheraga, *Biophys. Chem.* 59 (3) (1996) 329–339.
- [13] F. Solis, R. Wets, *Math. Oper. Res.* 6 (1) (1981) 19–30.
- [14] D. Delamarre, B. Viot, *RAIRO. Rech. Opér.* 32 (1) (1998) 43–73.
- [15] K. Doll, J.C. Schön, M. Jansen, *Phys. Chem. Chem. Phys.* 9 (46) (2007) 6128–6133.
- [16] K. Doll, J. Schön, M. Jansen, *Phys. Rev. B* 78 (14) (2008) 144110.
- [17] J. Pannetier, J. Bassas-Alsina, *Nature* 346 (26) (1990) 343–345.
- [18] H. Putz, J.C. Schön, M. Jansen, *J. Appl. Crystallogr.* 32 (5) (1999) 864–870.

- [19] P. Salamon, P. Sibani, R. Frost, Facts, Conjectures, and Improvements for Simulated Annealing, Society for Industrial and Applied Mathematics, Philadelphia, 2002, pp. 53–103.
- [20] J. Schön, M. Jansen, Ber. Bunsenges. Phys. Chem. (1994) 1541–1544.
- [21] M. Wevers, J. Schön, M. Jansen, J. Solid State Chem. 246 (136) (1998) 233–246.
- [22] K. Bao, S. Goedecker, K. Koga, F. Lançon, A. Neelov, Phys. Rev. B 79 (4) (2009) 041405.
- [23] S. Goedecker, J. Chem. Phys. 120 (21) (2004) 9911–9917.
- [24] S. Roy, S. Goedecker, V. Hellmann, Phys. Rev. E 77 (5) (2008) 056707.
- [25] S.E. Schönborn, S. Goedecker, S. Roy, A.R. Oganov, J. Chem. Phys. 130 (14) (2009) 144108.
- [26] B. Doliwa, A. Heuer, Phys. Rev. E 67 (3) (2003) 030501.
- [27] R. Gehrke, K. Reuter, Phys. Rev. B 79 (8) (2009) 085412.
- [28] H.G. Kim, S.K. Choi, H.M. Lee, J. Chem. Phys. 128 (14) (2008) 144702.
- [29] B. Olson, A. Shehu, Efficient basin hopping in the protein energy surface, in: 2012 IEEE Int. Conf. Bioinforma. Biomed., October 2012, pp. 1–6.
- [30] A. Verma, A. Schug, K.H. Lee, W. Wenzel, J. Chem. Phys. 124 (4) (2006) 044515.
- [31] D. Wales, J. Doye, J. Phys. Chem. A 5639 (97) (1997) 5111–5116.
- [32] D.J. Wales, Science 285 (5432) (1999) 1368–1372.
- [33] R. White, H. Mayne, Chem. Phys. Lett. 289 (1998) 463–468.
- [34] D. Deaven, K. Ho, Phys. Rev. Lett. 75 (2) (1995) 288–291.
- [35] C. Jiang, D. Morgan, I. Szlufarska, Phys. Rev. B 86 (14) (2012) 144118.
- [36] C. Jiang, D. Morgan, I. Szlufarska, Acta Mater. 62 (2014) 162–172.
- [37] R.L. Johnston, Dalton Trans. 22 (2003) 4193.
- [38] M.S. Bailey, N.T. Wilson, C. Roberts, R.L. Johnston, Eur. Phys. J. D – At. Mol. Opt. Phys. 25 (1) (2003) 41–55.
- [39] B. Hartke, Appl. Evol. Comput. Chem. 110 (2004) 33–53.
- [40] J.M. Dieterich, B. Hartke, Mol. Phys. 108 (3–4) (2010) 279–291.
- [41] N. Dugan, Ş. Erkoç, Comput. Mater. Sci. 45 (1) (2009) 127–132.
- [42] M. Sierka, Prog. Surf. Sci. 85 (9–12) (2010) 398–434.
- [43] B.C. Revard, W.W. Tipton, R.G. Hennig, Pred. Calculation Cryst. Struct. Top. Curr. Chem. 345 (2014) 181–222.
- [44] C.W. Glass, A.R. Oganov, N. Hansen, Comput. Phys. Commun. 175 (11–12) (2006) 713–720.
- [45] G. Johansson, T. Bligaard, A. Ruban, Phys. Rev. Lett. 88 (25) (2002) 1–5.
- [46] A.R. Oganov, Y. Ma, A.O. Lyakhov, M. Valle, C. Gatti, Rev. Mineral. Geochem. 71 (1) (2010) 271–298.
- [47] A.R. Oganov, C.W. Glass, J. Chem. Phys. 124 (24) (2006) 244704.
- [48] G. Trimarchi, A. Zunger, Phys. Rev. B 75 (10) (2007) 1–8.
- [49] G. Trimarchi, A. Freeman, A. Zunger, Phys. Rev. B 80 (9) (2009) 092101.
- [50] S. Woodley, Appl. Evol. Comput. Chem. 110 (2004) 95–132.
- [51] S.M. Woodley, R. Catlow, Nat. Mater. 7 (12) (2008) 937–946.
- [52] A.L.-S. Chua, N.A. Benedek, L. Chen, M.W. Finnis, A.P. Sutton, Nat. Mater. 9 (5) (2010) 418–422.
- [53] J. Zhang, C.-Z. Wang, K.-M. Ho, Phys. Rev. B 80 (17) (2009) 174102.
- [54] R. Briggs, C. Ciobanu, Phys. Rev. B 75 (19) (2007) 195415.
- [55] F.C. Chuang, C.V. Ciobanu, V.B. Shenoy, C.Z. Wang, K.M. Ho, Surf. Sci. 573 (2) (2004) L375–L381.
- [56] F.-C. Chuang, C.V. Ciobanu, C.-Z. Wang, K.-M. Ho, J. Appl. Phys. 98 (7) (2005) 073507.
- [57] D.C. Sayle, R.L. Johnston, Curr. Opin. Solid State Mater. Sci. 7 (1) (2003) 3–12.
- [58] S. Plimpton, J. Comput. Phys. 117 (1995) 1–42 (June 1994).
- [59] M. Hutter, Fitness uniform selection to preserve genetic diversity, in: Evolutionary Computation, 2002. CEC'02. Proceedings of the 2002 Congress, January, 2002.
- [60] T. Angsten, T. Mayeshiba, H. Wu, D. Morgan, New J. Phys. 16 (1) (2014) 015018.
- [61] S. Bahn, K. Jacobsen, Comput. Sci. Eng. (2002) 56–66.
- [62] D. Petti, J. Buongiorno, J. Maki, Nucl. Eng. Des. 222 (2003) 281–297.
- [63] G. Lucas, M. Bertolus, L. Pizzagalli, J. Phys.: Condens. Matter 22 (3) (2010) 035802.
- [64] Y. Watanabe, K. Morishita, A. Kohyama, J. Nucl. Mater. 417 (1–3) (2011) 1119–1122.
- [65] M. Bockstedte, A. Mattausch, O. Pankratov, Phys. Rev. B 69 (23) (2004) 1–13.
- [66] F. Gao, E. Bylaska, W. Weber, L. Corrales, Phys. Rev. B 64 (24) (2001) 245208.
- [67] H. Huangts, N.M. Ghoniem, J.K. Wongt, Modell. Simul. Mater. Sci. Eng. 3 (1995) 615–627.
- [68] J.M. Lento, L. Torpo, T.E.M. Staab, R.M. Nieminen, J. Phys.: Condens. Matter 16 (7) (2004) 1053–1060.
- [69] A. Mattausch, M. Bockstedte, O. Pankratov, Phys. Rev. B 70 (23) (2004) 235211.
- [70] Y. Watanabe, K. Morishita, Y. Yamamoto, Nucl. Instrum. Methods Phys. Res., Sect. B 269 (14) (2011) 1698–1701.
- [71] M.-J. Zheng, N. Swaminathan, D. Morgan, I. Szlufarska, Phys. Rev. B 88 (5) (2013) 054105.
- [72] F. Gao, D. Bacon, Y. Osetsky, J. Nucl. Mater. 276 (2000) 213–220.
- [73] R.A. Johnson, Phys. Rev. A 134 (5) (1964) 1329–1336.
- [74] L. Malerba, G.J. Ackland, C.S. Becquart, G. Bonny, C. Domain, S.L. Dudarev, C.-C. Fu, D. Hepburn, M.C. Marinica, P. Olsson, R.C. Pasianot, J.M. Raulot, F. Soisson, D. Terentyev, E. Vincent, F. Willaime, J. Nucl. Mater. 406 (1) (2010) 7–18.
- [75] L. Malerba, M.C. Marinica, N. Anento, C. Björkas, H. Nguyen, C. Domain, F. Djurabekova, P. Olsson, K. Nordlund, A. Serra, D. Terentyev, F. Willaime, C.S. Becquart, J. Nucl. Mater. 406 (1) (2010) 19–38.
- [76] M.-C. Marinica, F. Willaime, J.-P. Crocombette, Phys. Rev. Lett. 108 (2) (2012) 025501.
- [77] M.-C. Marinica, F. Willaime, N. Mousseau, Phys. Rev. B 83 (9) (2011) 094119.
- [78] Y. Osetsky, D. Bacon, A. Serra, B. Singh, S. Golubov, J. Nucl. Mater. 276 (1–3) (2000) 65–77.
- [79] R. Stoller, G. Odette, B. Wirth, J. Nucl. Mater. 251 (1997) 49–60.
- [80] D. Terentyev, T. Klaver, P. Olsson, M.-C. Marinica, F. Willaime, C. Domain, L. Malerba, Phys. Rev. Lett. 100 (14) (2008) 145503.
- [81] D. Terentyev, L. Malerba, M. Hou, Phys. Rev. B 75 (10) (2007) 104108.
- [82] F. Willaime, C.C. Fu, M.C. Marinica, J. Dalla Torre, Nucl. Instrum. Methods Phys. Res., Sect. B 228 (1–4) (2005) 92–99.
- [83] B.D. Wirth, G.R. Odette, D. Maroudas, G.E. Lucas, J. Nucl. Mater. 244 (3) (1997) 185–194.
- [84] G.J. Ackland, M.I. Mendelev, D.J. Srolovitz, S. Han, A.V. Barashev, J. Phys.: Condens. Matter 16 (27) (2004) S2629–S2642.
- [85] E. del Rio, J.M. Sampedro, H. Dogo, M.J. Caturia, M. Caro, A. Caro, J.M. Perlado, J. Nucl. Mater. 408 (1) (2011) 18–24.
- [86] A. Stukowski, B. Sadigh, P. Erhart, A. Caro, Modell. Simul. Mater. Sci. Eng. 17 (7) (2009) 075005.
- [87] T. Klaver, P. Olsson, M. Finnis, Phys. Rev. B 76 (21) (2007) 214110.
- [88] T.P.C. Klaver, G. Bonny, P. Olsson, D. Terentyev, Modell. Simul. Mater. Sci. Eng. 18 (7) (2010) 075004.
- [89] P. Olsson, C. Domain, J. Wallenius, Phys. Rev. B 75 (1) (2007) 014110.
- [90] J.M. Sampedro, E. del Rio, M.J. Caturia, M. Victoria, J. Manuel Perlado, J. Nucl. Mater. 417 (1–3) (2011) 1050–1053.
- [91] D. Terentyev, P. Olsson, T.P.C. Klaver, L. Malerba, Comput. Mater. Sci. 43 (4) (2008) 1183–1192.
- [92] D. Terentyev, L. Malerba, P. Klaver, P. Olsson, Joint Int. Top. Meet. Math. Comput. Supercomput. Nucl. Appl. (2007) 1–6.
- [93] J. Wang, G. Wang, J. Zhao, Chem. Phys. Lett. 380 (5–6) (2003) 716–720.